Journal of Alloys and Compounds 509 (2011) 9456–9459

Contents lists available at ScienceDirect

Journal of Alloys and Compounds

journal homepage: www.elsevier.com/locate/jallcom

Effect of polyethyleneimine on the growth of ZnO nanorod arrays and their application in dye-sensitized solar cells

Qiuliu Huang[a], Liang Fang[a,*], Xia Chen[b], Muhammad Saleem[a]

[a] State Key Laboratory of Power Transmission Equipment & System Security and New Technology, College of Physics, Chongqing University, Chongqing 400044, PR China
[b] College of Material Science and Engineering, Chongqing University of Technology, Chongqing 400054, PR China

ARTICLE INFO

Article history:
Received 16 May 2011
Received in revised form 9 July 2011
Accepted 11 July 2011
Available online 23 July 2011

Keywords:
ZnO nanorod
Polyethyleneimine (PEI)
Dye-sensitized solar cells
Photovoltaic performance

ABSTRACT

A series of oriented hexagonal wurtzite ZnO nanorod-array films were grown on fluorine-doped tin oxide (FTO) coated glass substrates by chemical process. The effect of polyethyleneimine (PEI) on the structure and micro-morphology of ZnO nanorod array films, as well as the photoelectric conversion properties in dye-sensitized solar cells (DSSCs) was analyzed. It was found that with the addition of PEI in growth solution, the ZnO nanorods became smaller in diameter and longer in length and hence the dye absorption and the photovoltaic performance of DSSCs were improved. A power conversion efficiency of 2.30% had been achieved on a DSSC based on a 7.9 μm-long nanorod array film prepared by a growth solution containing the PEI.

1. Introduction

ZnO has attracted much attention due to its piezoelectric [1–5], thermoelectric [6,7], electrical and optical properties [8–11]. In the field of energy conversion, due to the similarity of the energy band gap (3.37 eV at 298 K) and the electron-injection process of ZnO to that of TiO_2 [12], ZnO-based dye-sensitized solar cells (DSSCs) have attracted considerable interesting during the past several years. Furthermore, because of its higher electronic mobility and easier synthetic process, ZnO has been expected to be compatible with TiO_2 as a working electrode in DSSCs [13]. Recently, DSSCs based on one-dimensional (1-D) nanostructures including nanowires or nanorods have been fabricated due to the fast electron transport [14–20] in oriented single crystalline ZnO nanowire or nanorod arrays. However, a major drawback is to obtain long wires or rods [21]. It is reported that the additive such as polyethyleneimine (PEI) can increase the aspect ratio, which could increase the surface area for dye adsorption [22].

Herein, the ZnO nanorod-array films were grown on FTO substrates by chemical process including the preparation of seed layer using ZnO sol and the growth of ZnO nanorods. In this process, the PEI was added in ZnO sol and the growth solution, respectively. The effect of PEI on the structure and micro-morphology of ZnO nanorod array films, as well as the photoelectric conversion properties in dye-sensitized solar cells was discussed.

2. Experimental

2.1. Preparation and characterization of ZnO nanorod arrays

All of the solvents and chemicals used in this study were of reagent grade. Four pieces of fluorine-doped SnO_2 (FTO) substrates (i.e. **1**, **2**, **3**, and **4**) were ultrasonically cleaned in acetone and then cleaned with deionized water, respectively for 30 min. The following describes the specific experimental procedure for rapid growth of ZnO nanorods. Firstly, the substrates **1** and **2** were spin coated with the ZnO sol of 0.005 M zinc acetate in ethanol; while the substrates **3** and **4** were spin coated with the ZnO sol of 0.005 M zinc acetate and 0.005 mM PEI (molecular weight 70,000, Aladdin) in ethanol. Then the four substrates coated with ZnO sol were treated at 380 °C for 1 h to form ZnO nanocrystals on the surface of the substrates by thermal decomposition of zinc acetate, and these ZnO nanocrystals were used as seeds for subsequent growth of ZnO nanorods. Next, two growth solutions **A** and **B** were prepared. The solution **A** consisted of 0.025 M zinc acetate, and 0.025 M hexamethylenetetramine (HMTA) in deionized water; while the solution **B** included 0.025 M zinc acetate, 0.025 M HMTA, and 0.005 mM PEI in deionized water. The seeded substrates **1** and **3** were then placed vertically in 40 mL of the solution **A**; while substrates **2** and **4** were in the solution **B** with the same volume as the solution **A**. This reaction was carried out at 90 °C for 12 h. During the growth process, whole solutions were replaced every 3 h. After the reaction, the four films were taken out to rinse with deionized water for several times and annealed in air at 450 °C for 30 min to remove any residual organics. The preparation conditions for ZnO nanorod array films **1**–**4** were described in Table 1.

The crystal structure of the films was characterized by X-ray diffraction (Bruker D8 with Cu Kα radiation, λ = 1.5406 Å) from 20° to 80° at a scanning speed of 8° min^{-1}. The surface morphology of the films was observed on scanning electron

* Corresponding author at: College of Physics, Chongqing University, Chongqing 400044, PR China. Tel.: +86 23 65678369.
E-mail addresses: huangqiuliu@126.com(Q. Huang),fangliangcqu@yahoo.com.cn (L. Fang).

0925-8388/$ – see front matter © 2011 Elsevier B.V. All rights reserved.
doi:10.1016/j.jallcom.2011.07.029

Table 1
Preparation conditions for ZnO nanorod array films **1**–**4**.

Films	ZnO sol	Growth solution
1	Without PEI	Without PEI
2	Without PEI	With PEI
3	With PEI	Without PEI
4	With PEI	With PEI

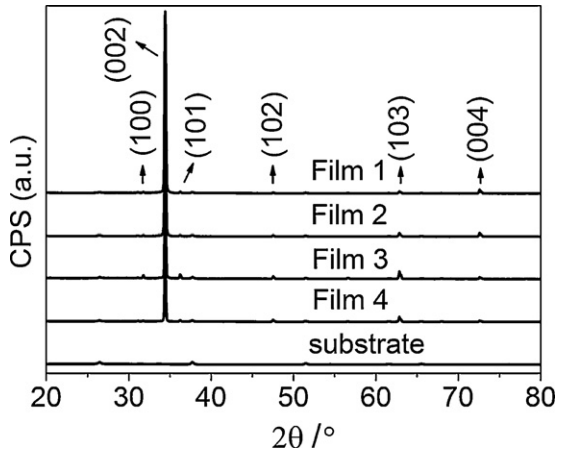

Fig. 1. XRD patterns of FTO substrate and the ZnO films **1**–**4** on FTO substrate.

microscopy (SEM, XL 30). The thickness of the films was measured by a step profiler (Dektak 150).

2.2. Fabrication and photovoltaic measurement of DSSCs

To fabricate DSSCs, the ZnO nanorod array films were limited to 0.25 cm^2 by removing extra nanorods with a blade. The films were sensitized by immersing in 0.3 mM 2-cyano-3-{5′-[1-cyano-2-(1,1,6,6-tetramethyl-10-oxo-2,3,5,6-tetrahydro-*1H*,*4H*,*10H*-11-oxa-3a-aza-benzo[*de*]anthracen-9-yl)-vinyl]-[2,2′]bithiophenyl-5-yl}-acrylic acid (NKX-2883) [23] in ethanol for 24 h to complete the dye adsorption. The DSSCs were fabricated by assembling the dye-sensitized films as the working electrode and Pt-coated FTO as the counter electrode, separated with a 30 μm hot-melt surlyn film. A solution consisting of 0.1 M LiI, 0.05 M I_2, 0.6 M 1, 2-dimethyl-3-n-propylimidazolium iodide, and 0.1 M 4-*tert*-butylpyridine in acetonitrile was introduced into the space between the working electrode and counter electrode through capillary. The photovoltaic performance of DSSC was tested by recording the *J*–*V* curves with a Keithley 2400 Source Meter under 100 mW/cm^2 AM 1.5G simulated sunlight coming from a solar simulator (Oriel-91193) equipped with a 1000 W Xe lamp and an AM 1.5 filter. The light intensity was calibrated using a Si solar cell (Oriel-91150). A black mask with aperture area of 0.2304 cm^2 was used to avoid stray light during measurement. Incident monochromatic photon-to-electron conversion efficiency (IPCE) measurements were conducted using an Oriel-74125 system (Newport), and the intensity of monochromatic light was measured with a Si detector (Oriel-71640).

3. Results and discussion

3.1. Structural and morphological characterization

Fig. 1 shows the XRD patterns of the as-grown films **1**–**4**. All the films exhibit the diffraction peaks of (1 0 0), (0 0 2), (1 0 1), (1 0 2), (1 0 3), and (0 0 4), which is consistent with the hexagonal wurtzite phase of ZnO, indicating that the PEI added in ZnO sol or growth solution has no effect on the structure of ZnO films. Besides, the intensity of the (0 0 2) diffraction peak is much stronger than that of other peaks, which is different from the power XRD profile where the (0 0 2) peak is not the strongest. It means the as-grown ZnO films are oriented on the substrate surface along the [0 0 1] growth direction.

The above films were further observed on scanning electron microscopy. Fig. 2 displays the SEM images of the top views and 30° tilted views for films **1**–**4**. The diameter of films **1**–**4** is 278, 173, 382, 191 nm, respectively, and the length of these films obtained by the step profiler is 6.1, 7.9, 8.1, 9.7 μm, respectively, which were listed in Table 2. For the samples obtained from the same growth solution (i.e. films **1** and **3** or films **2** and **4**), the nanorods were sparser, and stood at different angles to the substrate surface normal and had larger diameter when adding PEI in ZnO sol; while the nanorods obtained by the condition without PEI in ZnO sol were uniform, dense, and relatively small in diameter. In addition, for the films prepared by the similarly seeded substrate (i.e. films **1** and **2** or films **3** and **4**), it was found that with the addition of PEI in growth solution the nanorods were smaller in diameter and longer in length than those prepared without PEI in growth solution. According to the above observations, the preparation condition with PEI in growth solution but without PEI in ZnO sol was the best for the growth of oriented and long nanorod array on the FTO substrate.

3.2. Growth mechanism of ZnO nanorods

In the typical synthesized process, ZnO nanorods were prepared based on the following reaction [24]:

$$Zn^{2+} + 2OH^- \rightarrow Zn(OH)_2 \rightarrow ZnO + H_2OorZn^{2+} + 2OH^-$$
$$\rightarrow ZnO + H_2O$$

In this study, zinc acetate was the precursor, and HMTA was used as the hydroxide source. The growth of ZnO nanorods was conducted by two steps: (1) the formation of crystal nucleus as seeds by spin coating process with ZnO sol, and (2) the formation and growth of the nanorods, as shown in Fig. 3. It is easy to synthesize one-dimensional ZnO structure since the crystal plane (0 0 1) of ZnO which has the highest surface energy of the low-index surfaces possesses smaller activation energy for nucleation and faster growth velocity than other crystal planes [25]. The growth of oriented ZnO nanorods was also induced by the seeds which were the stationary and evenly distributed nucleation centers on the surface of the substrate. If more crystal nucleus formed on the surface of FTO substrate, the as-grown nanorods would closely arrange owing to Steric Effect [26] that caused the nanorods grow along the vertical direction to the substrate and suppressed the oblique direction. However, when adding PEI in ZnO sol, the colloidal particles reunited and even precipitated due to the increased alkalinity, which resulted in relatively less crystal nucleus and consequently sparser and more oblique nanorods with larger diameter as the nanorods in films **3** and **4**. Meanwhile, the thickness of films **3** and **4** was more than that of films **1** and **2** due to the less crystal nucleus in the growth solution with the same concentration of Zn^{2+}. Furthermore, PEI could preferentially adsorb to different crystal faces, modifying the surface free energy and growth rate [22], and it can inhabit radial growth but allow axial growth of the nascent nanorods, consequently increasing the aspect ratios of

Table 2
Average photovoltaic performance parameters for the DSSCs based on ZnO nanorod array films **1**–**4**.

Film	Diameter [nm]	Thickness [μm]	J_{sc} [mA cm^{-2}]	V_{oc} [V]	*FF*	η [%]
1	278	6.1	5.84 ± 0.019	0.503 ± 0.003	0.539 ± 0.004	1.58 ± 0.003
2	173	7.9	7.30 ± 0.067	0.577 ± 0.004	0.546 ± 0.004	2.30 ± 0.014
3	382	8.1	4.64 ± 0.033	0.523 ± 0.002	0.507 ± 0.005	1.23 ± 0.002
4	191	9.7	4.83 ± 0.067	0.543 ± 0.004	0.574 ± 0.004	1.51 ± 0.023

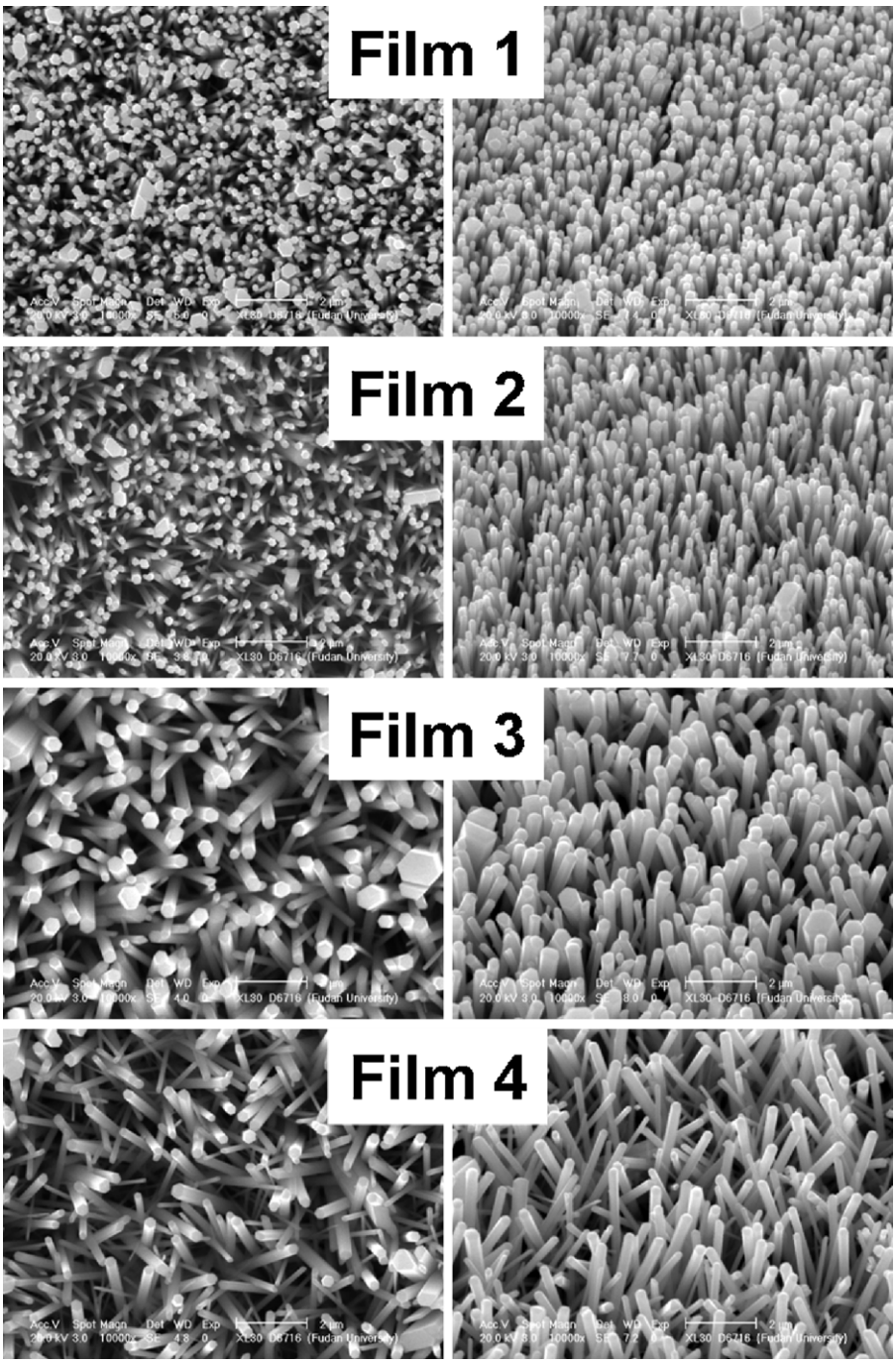

Fig. 2. SEM images of the top views (left) and 30° tilted views (right) for films **1**–**4**.

nanorods. As a result, with adding the PEI in the growth solution, longer ZnO nanorods with smaller diameter were obtained.

3.3. Solar cell performance

The *J*–*V* characteristics of the DSSCs assembled using the above films **1**–**4** were compared in Fig. 4 and the average photovoltaic data were summarized in Table 2. The DSSC based on film **1** produced η of 1.58% (J_{sc} = 5.84 mA cm^{-2}), while the DSSC based on film **2** produced η of 2.30% (J_{sc} = 7.30 mA cm^{-2}), which is comparable with the η of 2.10% obtained from the DSSC based on a 33 μm-long ZnO nanowire by Xu et al. [21]. The improved power conversation efficiency of 45% was induced by the increased length of nanorods from 6.1 μm (film **1**) to 7.9 μm (film **2**); this also can be conformed by the comparison of films **3** and **4**. As the nanorods got longer with adding PEI in growth solution, the dye adsorption would be increased, and thus the J_{sc} and η would be improved. However, the DSSCs based on film **4** obtained when adding the PEI in ZnO sol had lower η than film **2**

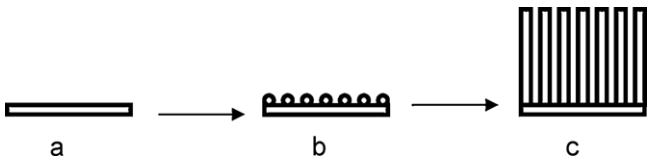

Fig. 3. Growth process of ZnO nanorods on FTO substrate. (a) FTO substrate; (b) seed layer on FTO substrate; and (c) nanorods on FTO substrate.

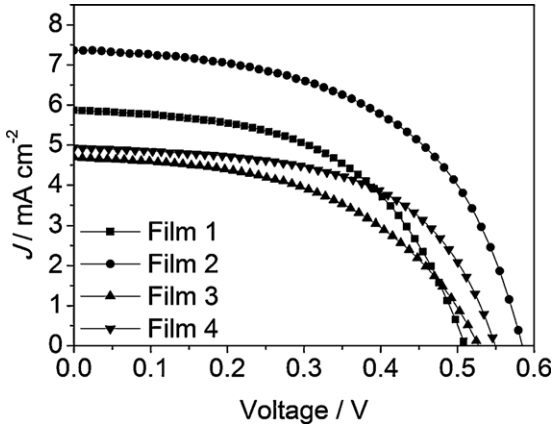

Fig. 4. *J–V* curves of the DSSCs assembled respectively from films **1**–**4** under simulated AM 1.5G solar light (100 mW cm^{-2}).

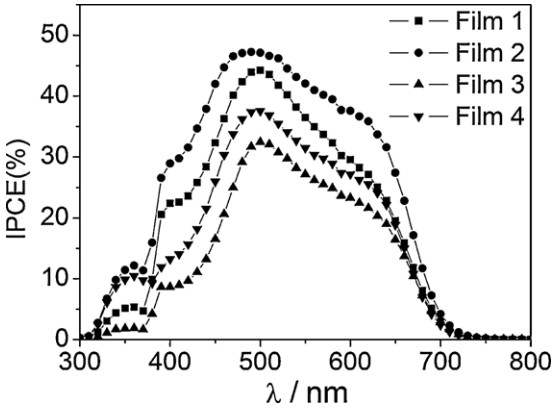

Fig. 5. IPCE spectra of the DSSCs assembled respectively from films **1**–**4**.

due to the smaller J_{sc}. Though the thickness of film **4** was more than that of film **2**, the nanorods in film **4** were a little oblique instead of being well aligned as film **2**, which would decrease the electron transportation in nanorod films; and the competition of the two aspects induced the decrease of the J_{sc}.

Fig. 5 shows the IPCE spectra of DSSCs based on films **1**–**4**. The IPCE value at 500 nm was 44.2% for the DSSC based on Film 1, while 47.1% for the DSSC based on film **2**, evidently, the improved IPCE was attributed to the enhancement of dye adsorption which was resulted from the increased length of the nanorods. For films **3** and **4**, the IPCE value at 500 nm was 32.4% and 37.5%, respectively, which was relatively lower than that of DSSC based on film **2**. These were in accord with the J_{sc} results.

4. Conclusions

In summary, the oriented hexagonal wurtzite ZnO nanorod array films were successfully prepared on FTO substrates by chemical process. It was found that the addition of PEI had much effect on the structure and micro-morphology of ZnO nanorod array films, as well as the photoelectric conversion properties in DSSCs. With adding the PEI in ZnO sol, the as-prepared ZnO nanorods were sparser and more oblique; while with PEI in the growth solution, the nanorods became smaller in diameter and longer in length and hence the dye absorption and the photovoltaic performance of DSSCs were improved. A power conversion efficiency of 2.30% had been achieved on a DSSC based on a 7.9 μm-long nanorod array film prepared by a growth solution containing the PEI.

Acknowledgements

This work was financially supported by the National Natural Science Foundation of China (Grant Nos. 11074314 and 50942021), the Fundamental Research Funds for the Central Universities No. CDJXS10102207, the Visiting Scholarship of State Key Laboratory of Power Transmission Equipment & System Security and New Technology (2007DA10512711403), the Third Stage of 211 Innovative Talent Training Project (S-09109) and Sharing Fund of Large-scale Equipment of Chongqing University (Grant Nos. 2010063072 and 2010121556). The author (Qiuliu Huang) will thank Prof. Wang Z S's research group at Fudan University for their kind help and suggestion during the solar cell performance experiment.

References

[1] M. Li, Y.J. Su, W.Y. Chu, L.J. Qiao, A.A. Volinsky, G. Kravchenko, Appl. Phys. Lett. 98 (2011) 082105.
[2] M.-S. Cao, D.-W. Wang, J. Yuan, H.-B. Lin, Q.-L. Zhao, W.-L. Song, D.-Q. Zhang, Mater. Lett. 64 (2010) 1798–1801.
[3] Z.Z. Shao, L.Y. Wen, D.M. Wu, X.A. Zhang, S.L. Chang, S.Q. Qin, J. Appl. Phys. 108 (2010) 124312.
[4] J.W.C Wang, J. Alloys Compd. 449 (2008) 44–47.
[5] X.R. Qu, W. Wang, S.C. Lv, D.C. Jia, Solid State Commun. 151 (2011) 332–336.
[6] Y. Kinemuchi, M. Mikami, K. Kobayashi, K. Watari, Y. Hotta, J. Electron. Mater. 39 (2010) 2059–2063.
[7] G.V. Prakash, K. Pradeesh, A. Kumar, R. Kumar, S.V. Rao, M.L. Markham, J.J. Baumberg, Mater. Lett. 62 (2008) 1183–1186.
[8] N. Gopalakrishnan, L. Balakrishnan, K. Latha, S. Gowrishankar, Cryst. Res. Technol. 46 (2011) 361–367.
[9] H. Tong, Z.H. Deng, Z.G. Liu, C.G. Huang, J.Q. Huang, H. Lan, C. Wang, Y.G. Cao, Appl. Surf. Sci. 257 (2011) 4906–4911.
[10] W.W. Zhong, F.M. Liu, L.G. Cai, C.C. Zhou, P. Ding, H. Zhang, J. Alloys Compd. 499 (2010) 265–268.
[11] H. Cheun, C. Fuentes-Hernandez, Y.H. Zhou, W.J. Potscavage, S.J. Kim, J. Shim, A. Dindar, B. Kippelen, J. Phys. Chem. C 114 (2010) 20713–20781.
[12] A. Furube, R. Katoh, T. Yoshihara, K. Hara, S. Murata, H. Arakawa, M. Tachiya, J. Phys. Chem. B 108 (2004) 12583–12592.
[13] C.H. Ku, J.J. Wu, Appl. Phys. Lett. 91 (2007) 93117.
[14] E. Galoppini, J. Rochford, H.H. Chen, G. Saraf, Y.C. Lu, A. Hagfeldt, G. Boschloo, J. Phys. Chem. B 110 (2006) 16159–16161.
[15] H.M. Gao, G.J. Fang, M.J. Wang, N.S. Liu, L.Y. Yuan, C. Li, L. Ai, J. Zhang, C.H. Zhou, S.J. Wu, X.Z. Zhao, Mater. Res. Bull. 43 (2008) 3345–3351.
[16] Y.M. Lee, H.W. Yang, J. Solid State Chem. 184 (2011) 615–623.
[17] J.J. Wu, G.R. Chen, H.H. Yang, C.H. Ku, J.Y. Lai, Appl. Phys. Lett. 90 (2007) 213109.
[18] A.J. Pai, B. Pradhan, S.K. Batabyal, Sol. Energ. Mat. Sol. C 91 (2007) 769–773.
[19] Y.F. Gao, M. Nagai, T.C. Chang, J.J. Shyue, Cryst. Growth Des. 7 (2007) 2467–2471.
[20] A. Qurashi, M.F. Hossain, M. Faiz, N. Tabet, M.W. Alam, N.K. Reddy, J. Alloys Compd. 503 (2010) L40–L43.
[21] C. Xu, P. Shin, L. Cao, D. Gao, J. Phys. Chem. C 114 (2010) 125–129.
[22] L.E. Greene, B.D. Yuhas, M. Law, D. Zitoun, P. Yang, Inorg. Chem. 45 (2006) 7535–7543.
[23] Z.-S. Wang, Y. Cui, K. Hara, Y. Dan-oh, C. Kasada, A. Shinpo, Adv. Mater. 19 (2007) 1138.
[24] J.G. Chen, C.X. Guo, L.L. Zhang, J.T. Hu, P. Guo, Chin. J. Luminescence 26 (2005) 83–88.
[25] Y. Tong, Y. Liu, L. Dong, D. Zhao, J. Zhang, Y. Lu, D. Shen, X. Fan, J. Phys. Chem. B 110 (2006) 20263–20267.
[26] Y. Tan, X. Xue, Q. Peng, H. Zhao, T. Wang, Y. Li, Nano Lett. 7 (2007) 3723–3738.